AGU PUBLICATIONS

JGR

Journal of Geophysical Research: Atmospheres

RESEARCH ARTICLE

10.1002/2014JD021677

Key Points:
- Studied L-A coupling over North America
- Impact of soil moisture state on extremes such as hot days and hot spells
- Interesting L-A coupling for climatologically nontransitional regions

Correspondence to:
G. T. Diro,
diro@sca.uqam.ca

Citation:
Diro, G. T., L. Sushama, A. Martynov, D. I. Jeong, D. Verseghy, and K. Winger (2014), Land-atmosphere coupling over North America in CRCM5, *J. Geophys. Res. Atmos.*, *119*, 11,955–11,972, doi:10.1002/2014JD021677.

Received 21 FEB 2014
Accepted 25 SEP 2014
Accepted article online 27 SEP 2014
Published online 8 NOV 2014

Land-atmosphere coupling over North America in CRCM5

G. T. Diro[1], L. Sushama[1], A. Martynov[1,2], D. I. Jeong[1], D. Verseghy[3], and K. Winger[1]

[1]Centre ESCER, University of Quebec at Montreal, Montreal, Quebec, Canada, [2]Institute of Geography and Oeschger Centre for Climate Change Research, University of Bern, Bern, Switzerland, [3]Climate Research Division, Environment Canada, Toronto, Ontario, Canada

Abstract Land-atmosphere coupling and its impact on extreme precipitation and temperature events over North America are studied using the fifth generation of the Canadian Regional Climate Model (CRCM5). To this effect, two 30 year long simulations, spanning the 1981–2010 period, with and without land-atmosphere coupling, have been performed with CRCM5, driven by the European Centre for Medium-Range Weather Forecasts reanalysis at the boundaries. In the coupled simulation, the soil moisture interacts freely with the atmosphere at each time step, while in the uncoupled simulation, soil moisture is replaced with its climatological value computed from the coupled simulation, thus suppressing the soil moisture-atmosphere interactions. Analyses of the coupled and uncoupled simulations, for the summer period, show strong soil moisture-temperature coupling over the Great Plains, consistent with previous studies. The maxima of soil moisture-precipitation coupling is more spread out and covers the semiarid regions of the western U.S. and parts of the Great Plains. However, the strength of soil moisture-precipitation coupling is found to be generally weaker than that of soil moisture-temperature coupling. The study clearly indicates that land-atmosphere coupling increases the interannual variability of the seasonal mean daily maximum temperature in the Great Plains. Land-atmosphere coupling is found to significantly modulate selected temperature extremes such as the number of hot days, frequency, and maximum duration of hot spells over the Great Plains. Results also suggest additional hot spots, where soil moisture modulates extreme events. These hot spots are located in the southeast U.S. for the hot days/hot spells and in the semiarid regions of the western U.S. for extreme wet spells. This study thus demonstrates that climatologically wet/dry regions can become hot spots of land-atmosphere coupling when the soil moisture decreases/increases to an intermediate transitional level where evapotranspiration becomes moisture sensitive and large enough to affect the climate.

1. Introduction

The increased recognition of the importance of land-atmosphere interactions and feedbacks in modulating the regional climate has led to several studies on this aspect in recent years [e.g., *Beljaars et al.*, 1996; *Eltahir*, 1998; *Schär et al.*, 1999; *Betts*, 2004; *Koster et al.*, 2006; *Guo et al.*, 2006; *Seneviratne et al.*, 2006; *Dirmeyer et al.*, 2006; *Mei et al.*, 2013]. The interaction between land surface and atmosphere is important because it could operate over a wide range of spatial and temporal scales. For instance, *Taylor et al.* [1997] demonstrated soil moisture-precipitation interaction at daily time scale and 10 km spatial scale over West Africa during the monsoon season, both in observations and models. Others [e.g., *Beljaars et al.*, 1996] have looked at interactions at a larger spatial scale and monthly to seasonal time scales. *Betts* [2004], for example, demonstrated the impact of soil moisture on monthly to seasonal rainfall and droughts over the U.S., while *Fischer et al.* [2007a, 2007b] studied the linkages between soil moisture and extreme hot spells over Europe. Some of the plausible links suggested in the above studies for the soil moisture-precipitation feedback is through the influence of high soil moisture in building up shallow planetary boundary layer (PBL) and increased latent heat flux into this shallow PBL. This enhanced evapotranspiration creates conducive environment for triggering more rainfall [*Schär et al.*, 1999]. On the other hand, the interaction of soil moisture and temperature is tied to the evaporative cooling associated with enhanced soil moisture, and therefore evapotranspiration, that will ultimately lead to reduced sensible heat and consequently to a decrease in temperature [*Seneviratne et al.*, 2010].

Although identifying the regions where land-atmosphere interactions are strong is important, it is difficult to investigate these using observations due to the lack of long-term records of soil moisture. Investigation of soil moisture-precipitation and soil moisture-temperature coupling, particularly the coupling strength

and regions of strong coupling, is therefore mostly based on global and regional climate models. However, the results from several modeling studies suggest that both the coupling strength and the regions of strong coupling are model dependent. For instance, *Koster et al.* [2006] and *Guo et al.* [2006], within the framework of the Global Land-Atmosphere Coupling Experiment (GLACE) using highly controlled seasonal simulations with 12 general circulation models (GCMs), quantified the importance of the land surface state, i.e., soil wetness, on boreal summer climate variability. Large spread in the land-atmosphere coupling strength was noted between the 12 participating models, which as discussed in *van den Hurk et al.* [2011], is used to illustrate the lack of understanding of the complex coupling process. Therefore, one of the aims of this study is to investigate and quantify the extent of land-atmosphere coupling, particularly soil moisture-temperature/precipitation coupling, over North America in the fifth generation of Canadian Regional Climate Model (CRCM5). This study will also explore the links between soil moisture and selected temperature and precipitation extremes such as the frequency and duration of hot spells and wet spells.

Fischer et al. [2007a] studied the impact of soil moisture on the impact of extreme hot days and hot spells over Europe and found that the land-atmosphere coupling increases the number of hot days in summer by 50 to 80%. Some other following studies such as *Fischer et al.* [2007b], *Hirschi et al.* [2010], *Jaeger and Seneviratne* [2011], and *Lorenz et al.* [2012] also focused on soil moisture impacts on extreme temperature events over Europe. Similar studies over North America include *Beljaars et al.* [1996] and *Betts* [2004] and are on the rise. However, these studies are all generally limited to the U.S., while the present study covers a wider part of North America.

The present study is based on two 30 year long simulations, with and without land-atmosphere coupling, spanning the 1981–2010 period, driven by European Centre for Medium-Range Weather Forecasts (ECMWF) reanalysis data at the lateral boundaries. In the coupled simulation the soil moisture is interactive, whereas in the second uncoupled simulation climatological values of soil moisture are prescribed at each grid point thus preventing the soil moisture-atmosphere interaction. The difference in the atmospheric variability between the two integrations will therefore be solely due to soil moisture-atmosphere interaction.

The paper is organized as follows. Section 2 presents the model, design of experiments, data, and methodology. Section 3 presents validation of coupled simulation in representing basic climatic features of the regions that are relevant to the present study. Sections 4 and 5 discuss the impact of soil moisture on the interannual variability of temperature and precipitation as well as its impact on extreme temperature and precipitation characteristics. Finally, summary and conclusions of this study are presented in section 6.

2. Model, Data, and Methods

2.1. Model and Experimental Design

The regional climate model, CRCM5 used in this study, is based on the global environmental multiscale model [*Côté et al.*, 1998] and uses a nonhydrostatic dynamical core with a hybrid vertical coordinate. The numerical scheme is composed of a two time level, semi-Lagrangian, implicit scheme. More details on the model is available in *Martynov et al.* [2012], but a brief description of the physics parameterization is given here. Convective processes are represented in the model following *Kain and Fritsch* [1992] for deep convection and *Bélair et al.* [2005] for shallow convection. The resolvable large-scale precipitation is computed following *Sundqvist et al.* [1989]. Radiation is parametrized by Correlated K solar and terrestrial radiation of *Li and Barker* [2005]. The planetary boundary layer scheme follows *Benoit et al.* [1989] and *Delage* [1997], with some modifications as described in *Zadra et al.* [2012]. Lakes, both resolved and subgrid scale, are represented by the Flake model [*Mironov et al.*, 2005, 2010]. The land surface scheme in CRCM5 is the Canadian Land Surface Scheme (CLASS) [*Verseghy*, 1991; *Verseghy et al.*, 1993; *Verseghy*, 2009], which allows flexible soil layers configurations. CLASS includes prognostic equations for energy and water conservation for the soil layers and a thermally and hydrologically distinct snow pack where applicable. The thermal budget is performed over all layers, but the hydrological budget is done only for layers above the bedrock. In an attempt to crudely mimic subgrid-scale variability, CLASS adopts a pseudomosaic approach and divides the land fraction of each grid cell into a maximum of four subareas: bare soil, vegetation, snow over bare soil, and snow with vegetation. The energy and water budget equations are first solved for each subarea separately and then averaged over the grid cell, using averaged structural attributes and physiological properties of the four plant functional types in CLASS: needleleaf trees, broadleaf trees, crops, and grasses. These structural attributes include leaf area index, roughness length, canopy mass, and root depth, which have to be specified if they are present in a grid cell.

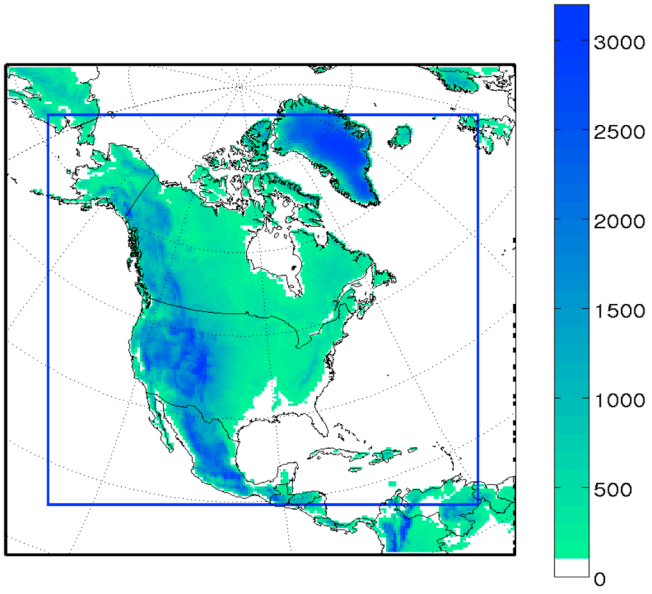

Figure 1. The computational domain with topography (m). The region enclosed by the blue box is the free domain.

Two simulations (coupled and uncoupled) were performed with CRCM5, using the same approach as in *Seneviratne et al.* [2006], to examine land-atmosphere coupling over North America. The coupled simulation is the same as in *Martynov et al.* [2013], which cover the 1958–2010 period, driven by ECMWF Re-Analysis (ERA-40) until 1978, followed by ERA-Interim [*Dee et al.*, 2011] till 2010. The land surface model configuration consists of 26 soil layers, extending up to 60 m. Sand and clay fields, as well as the bare soil albedo formula, follow ECOCLIMAP [*Masson et al.*, 2003]. The initial conditions for the soil temperature and moisture were produced from a 300 year CLASS offline simulation driven by climatological ERA-Interim data. In this study we analyze the 1981–2010 period of the simulation. The second simulation (the uncoupled run) is then carried out for 30 years from 1981 to 2010 (inclusive), similar to the coupled run, except that in this simulation the soil liquid and soil ice water content are replaced with climatological averages computed from the coupled run for the 1981–2010 period. Since the initial condition for the uncoupled run is taken from the last time step of year 1980 of the coupled simulation, differences between the coupled and uncoupled simulations will reflect the impact of land-atmosphere coupling.

The simulation domain (Figure 1) covers whole of North America and adjoining oceans. The model is configured with a 50 km (0.44°) horizontal resolution and 56 levels in the vertical with the top level near 10 hPa. It has to be noted that the horizontal spacing of 50 km is still too coarse to represent adequately the mesoscale convective systems. The model time step for this simulation is set to 20 min. The model domain has a total of 212 × 200 grid points including a 10 point halo and a 10 point blending zone for the process of merging the model results with the boundary fields. The remaining 172 × 160 inner grid points cover the region between 20°N–88°N and 30°W–150°W. Analysis is however carried out only over land grid points south of 60°N, i.e., southern Canada and contiguous U.S., as daily observations required in this study were available only for this region.

2.2. Data

The gridded daily observed rainfall and maximum temperature data used in this study were obtained from *Maurer et al.* [2002] for the U.S. and *Hutchinson et al.* [2009] and *Hopkinson et al.* [2011] for Canada. The U.S. data set has a spatial resolution of 0.125° and cover the contiguous United States. The Canadian data set covers the Canadian land mass south of 60°N and is available at 0.1° resolution. This gridded data set was developed from daily observations at Environment Canada climate stations, using a thin plate smoothing spline surface fitting method [*Hutchinson et al.*, 2009].

In the absence of observed evapotranspiration data, those from the Global Land Data Assimilation System (GLDAS) [*Rodell et al.*, 2004] are used in this study. GLDAS data are generated by forcing land surface model and assimilating the model simulation with data from the new generation of remotely sensed data set and are available at a resolution of 1 × 1°.

2.3. Methods

2.3.1. Coupling Strength Measures

Land-atmosphere coupling strength is evaluated using three methods: the variance method [*Seneviratne et al.*, 2006; *Zhang et al.*, 2008], the GLACE coupling parameter [*Koster et al.*, 2006], and the correlation method [*Seneviratne et al.*, 2006], which are discussed below. Since the focus of this study is on the boreal summer, only the June–August (JJA) months are analyzed.

1. In the variance method, the contribution of the interactive soil moisture to the interannual variability of the climatic variable v of interest is computed as $\Delta\sigma^2 v = \frac{\sigma^2_{\text{coupled}}v - \sigma^2_{\text{uncoupled}}v}{\sigma^2_{\text{coupled}}v}$, where $\sigma_{\text{coupled}}v$ and $\sigma_{\text{uncoupled}}v$ are the standard deviations of v for the coupled and uncoupled simulations, respectively. The seasonal (JJA) mean values are used in this analysis to focus on the interannual variability. Higher values of $\Delta\sigma^2 v$ imply strong contribution of land (soil moisture) on the interannual variability of the climate variable v.
2. The second method of measuring the coupling strength is using the GLACE-type coupling strength parameter (Ω). Unlike the variance method, this method measures the strength of the coupling at the subseasonal time scale. In this method the coupling of the land surface to the climate variable is given by : $\Delta\Omega_v = (\Omega_{\text{uncoupled}}v - \Omega_{\text{coupled}}v)$ and Ω_v is defined as $\Omega_v = \frac{N\sigma^2_{\hat{v}} - \sigma^2_v}{(N-1)\sigma^2_{\hat{v}}}$ where N is the number of ensemble members, σ^2_v is the variance of the 6 day total or mean of the climate variable in question computed from all available data (i.e., 30 years × number of 6 day mean or total in a season), and $\sigma^2_{\hat{v}}$ is the ensemble mean variance of the non overlapping 6 day mean or total. The 6 day mean is used for temperature, whereas the 6 day total is used for precipitation. The 6 day period is chosen to be consistent with *Koster et al.* [2006] to facilitate easy comparison. Similarly, to be consistent with the GLACE analysis period, the first 8 days of June are omitted and the June to August (JJA) period is divided into fourteen 6 day mean/total. It is important to note that the computation of Ω here is slightly different from *Koster et al.* [2006] due to the difference in the design of experiment, in particular with respect to the computation of the ensemble mean variance $\sigma^2_{\hat{v}}$. In this paper, as in *Seneviratne et al.* [2006] and *Tawfik and Steiner* [2011], the ensemble members (N) correspond to the 30 years.
3. The third method of measuring the land-atmosphere coupling strength is by using the correlation coefficient between temperature and evapotranspiration. As the computation of the correlation coefficient is based on the time series of the seasonal mean values of temperature and evapotranspiration, the estimated coupling strength is at the interannual time scale. Unlike the variance and GLACE-type methods, which are used for measuring both the soil moisture-temperature and soil moisture-precipitation coupling strength, the correlation method is used in this study to measure only the soil moisture-temperature coupling strength. Higher negative correlation values are suggestive of the high importance of soil moisture on the temperature variability. However, *Seneviratne et al.* [2006] noted that this measure is less meaningful for very dry regions where there is very little evapotranspiration.

2.3.2. Climate Extreme Indices

In this study, selected extreme temperature and precipitation indices are considered to explore the linkage between soil moisture and climate extremes. The extreme temperature indices considered are the number of hot days (NHDs), hot spell frequency (HSF), and maximum duration of hot spells (MxDHS). A hot day is defined as a day with daily maximum temperature above or equal to a predefined threshold. This predefined threshold is the long-term (1981–2010) 90th percentile of daily maximum temperature computed for each calendar day of the 92 days in JJA season, for each grid point. A hot spell is defined as three or more consecutive hot days. It must be noted that the consecutive days are nonoverlapping. The hot spell frequency (HSF) is the frequency of occurrence of hot spells, and the maximum hot spell duration (MxDHS) is the duration of the longest hot spell. For precipitation extremes, we consider the maximum duration of extreme wet spells (MxDWS). Extreme wet day is defined as a day with the daily mean precipitation above or equal to the long-term 90th percentile threshold. Similar to the threshold used to define the hot day, the long-term 90th percentile threshold is computed for each grid point and for each calendar day of the summer season. Extreme wet spell is defined as an event lasting three or more consecutive days. Consequently, MxDWS represents the longest duration of extreme wet spell.

Since soil moisture observations are not available, a commonly used proxy for soil moisture, the Standardized Precipitation Index (SPI) [*McKee et al.*, 1993], is used in this study. More specifically, SPI3, which uses the previous 3 month cumulative precipitation, is considered. To compute SPI3, a nonparametric kernel function is fitted to the cumulative precipitation values first to determine the probability density function [*Jeong et al.*, 2014], which is then used to obtain the corresponding cumulative distribution function (CDF). The final SPI3 is then obtained by mapping the CDF on to the standard normal distribution function.

3. Model Evaluation

Martynov et al. [2013] evaluated extensively the performance of CRCM5 over the same North American domain considered in this study against Climatic Research Unit, Global Precipitation Climatology Project,

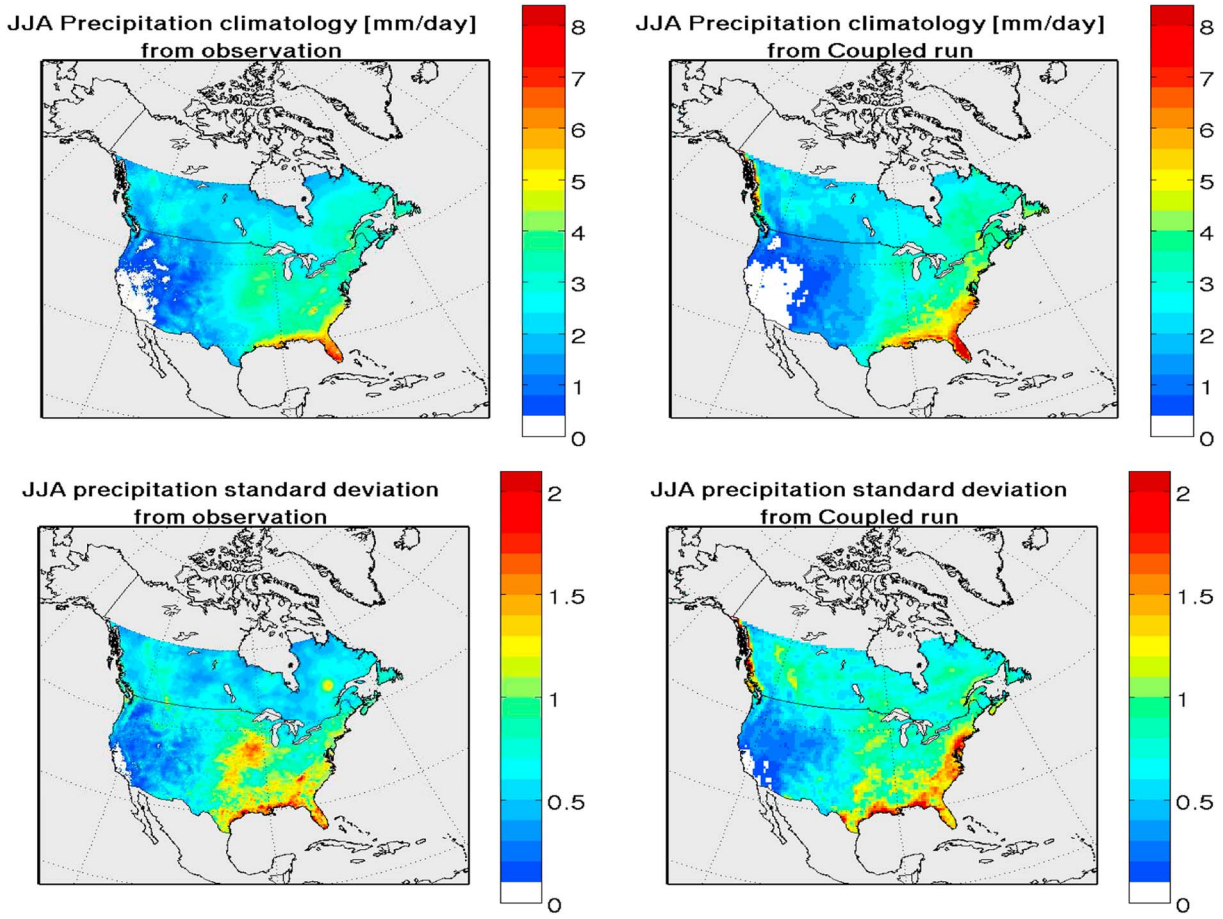

Figure 2. (top row) Mean and (bottom row) standard deviation of summer (JJA) precipitation (mm/d) from (left column) observations and (right column) coupled simulation of the model.

and University of Delaware data sets and found that the model reproduces reasonably well many aspects of the regional climate (diurnal, interannual, and intraannual variabilities). Therefore, only validation/performance of selected variables such as the daily maximum temperature and precipitation and their variability in the coupled simulation will be presented in this article.

The spatial distribution of modeled and observed mean and interannual variability of JJA precipitation is shown in Figure 2. The wet areas of eastern North America, particularly the southeastern U.S., and the semi-arid and arid western coastal areas are reproduced well by the model. This is reflected in the high value of spatial correlation, $r = 0.92$, between the coupled simulation and observation. The spatial pattern of the interannual variability roughly follows the pattern of the mean climatology, both in the observation and in the coupled simulation. The model reproduces the east-west gradient in the variability but underestimates the variability over the Central Great Plains and overestimates over the U.S. eastern coastal area. It must be noted that the Great Plains is one of the hot spots of land-atmosphere coupling according to the GLACE studies [*Koster et al.*, 2006].

Figure 3 shows the mean and interannual variability of the summer daily maximum temperature (T_{max}). The spatial correlation between simulated and observed temperatures is of the order of 0.96, suggesting that the spatial distribution of the seasonal mean values of T_{max} are reproduced well by the model. The variability, however, is overestimated by the model over the Great Plains (especially over the Southern Great Plains) and over the northern and northeastern limit of the study area. The maximum variability in the observational data set is located over Northern Great Plains and over central Canada. The model also shows the highest variability over the Great Plains and over central and northeastern Canada, though it is overestimated.

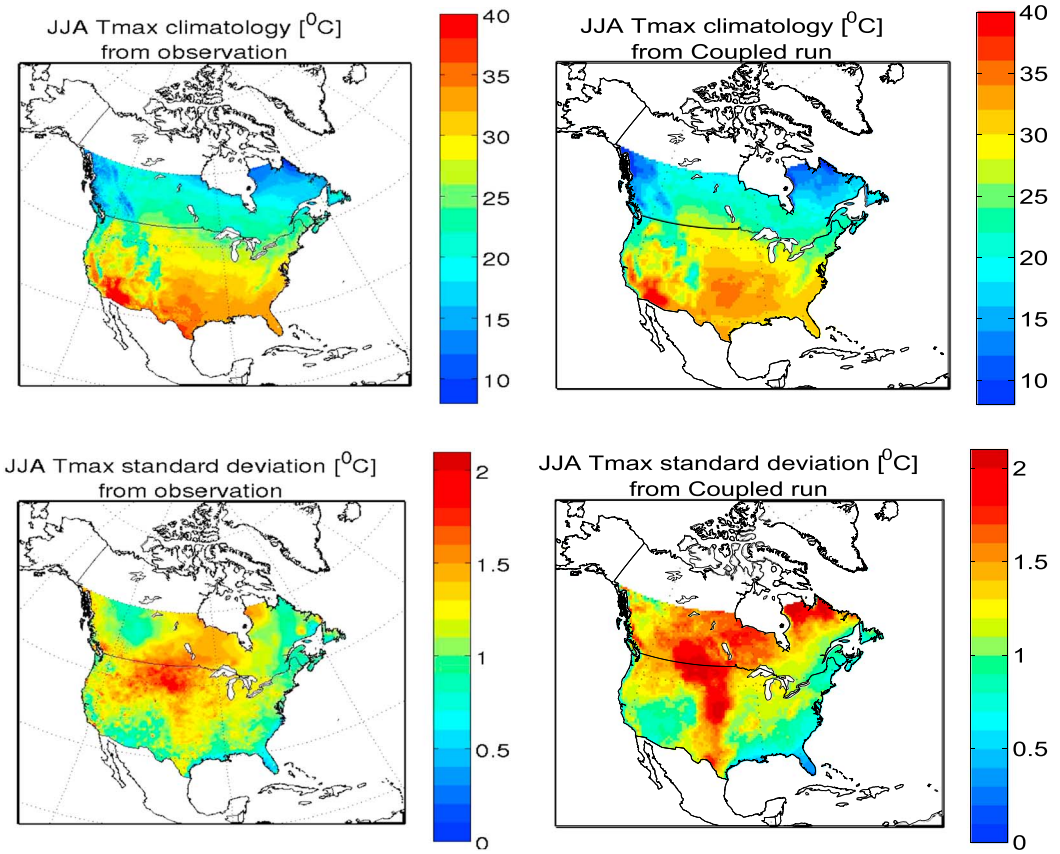

Figure 3. (top row) Mean and (bottom row) standard deviation of summer (JJA) maximum temperature (T_{max}) (°C) in the (left column) observation and (right column) coupled simulation.

The model's capability in reproducing most aspects of the observed characteristics reaffirms the use of this model as a tool for further investigation of the coupling strength in the model.

4. Soil Moisture-Temperature Coupling

In this section, the spatial distribution and strength of soil moisture-temperature coupling will be analyzed. Given that the land-atmosphere interaction is stronger during day time compared to night time as illustrated in past studies such as by *Zhang et al.* [2008], the daily maximum temperature (T_{max}) is used rather than the daily average for this analysis. Comparison of the interannual variability (IV) associated with the summer mean T_{max} from coupled and uncoupled simulations shows that the IV (as measured by the standard deviation) is reduced over the Great Plains in the uncoupled run (not shown), as a result of the suppression of the interannual variability of soil moisture. This increase/decrease in variability as a result of coupling/decoupling interannually varying soil moisture agrees with past studies of *Delworth and Manabe* [1989] and *Seneviratne et al.* [2006].

Figure 4 shows the soil moisture-temperature coupling strength computed using the percentage of variance and GLACE $\Delta\Omega$ methods for JJA. Higher values in both methods are observed over the central U.S. and Great Plains which are indications of strong soil moisture-temperature coupling. In the GLACE method, since Ω_v measures the degree of resemblance among the ensemble members of the same simulation,(i.e., coupled or uncoupled), the difference in Ω for the two simulations ($\Omega_{uncoupled} - \Omega_{coupled}$) will indicate the degree to which soil moisture coupling brings a change in the variable considered [*Koster et al.*, 2006]. For the GLACE method, the coupling strength reaches up to 0.2 over the Great Plains (Figure 4, right). The percentage of variance shown in Figure 4 (left) indicates that the soil moisture-temperature coupling explains a significant fraction (more than three-fourths) of the variability over the Southern Great Plains and around 65% over the Northern Great Plains.

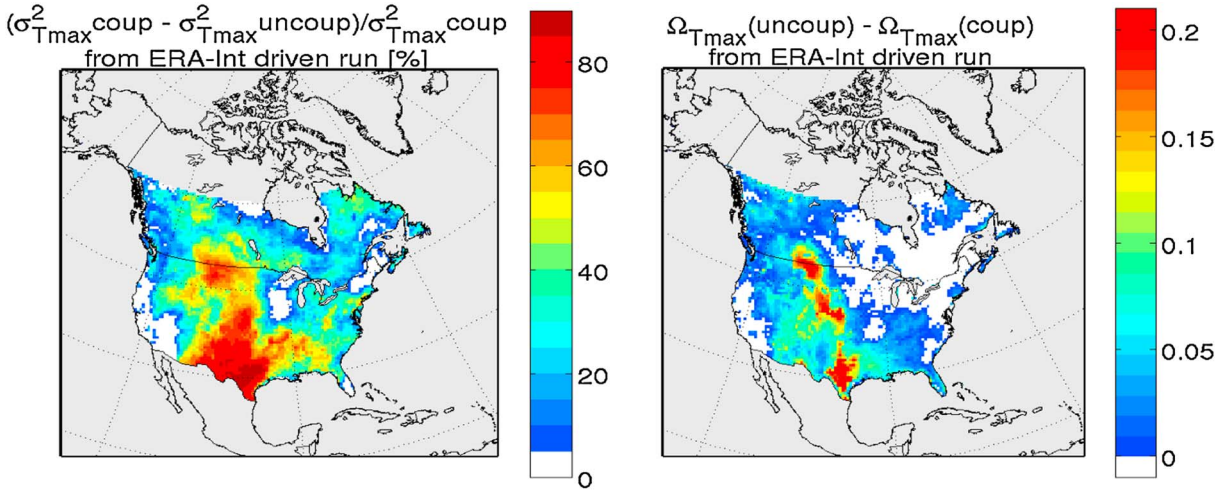

Figure 4. Soil moisture-temperature coupling strength as measured by (left) the percentage of variance and (right) GLACE $\Delta\Omega$ methods for summer (JJA) season.

The soil moisture is weakly associated with the daily maximum temperature over the Pacific coastal area, regions close to the Great Lakes, and over the northeastern regions of Canada (most of eastern Canada in $\Delta\Omega$ method). Past studies attributed this lack of soil moisture-temperature coupling to persistent lack of moisture or low evapotranspiration in the arid region of the southwest [*Karl*, 1986] and the advection of marine air by sea breezes in coastal area and regions closer to water bodies and lakes [*Walsh et al.*, 1985].

Both methods agree that the strongest soil moisture-temperature coupling occur over the transition region between the drier regions of the west and wetter regions of the east, which is in agreement with previous studies by *Koster et al.* [2006] and *Seneviratne et al.* [2006].

We further investigate the soil moisture-temperature coupling by computing the correlation coefficient between evapotranspiration and temperature as shown in Figure 5. The correlation between observed temperature and latent heat flux from GLDAS is negative over most parts of North America (except eastern Canada and western coast of Canada), with the maximum value located over the Great Plains. A strong negative correlation implies that the soil moisture controls the variability of evapotranspiration and temperature [*Seneviratne et al.*, 2006]. The positive correlation over eastern Canada and northeastern U.S. agrees well with the low coupling strength in the GLACE method, suggesting that the temperature variability for these regions is less influenced by the soil moisture variability. The coupled simulation also reproduces the negative correlation over the Great Plains, but significant differences can be noted over the southeastern U.S., where zero to positive correlation values are noted suggesting that the model interannual variability of temperature is less controlled by the soil moisture variability. Nevertheless, over most part of the domain, the model daily maximum temperature relates to the evapotranspiration the same way as in the observations.

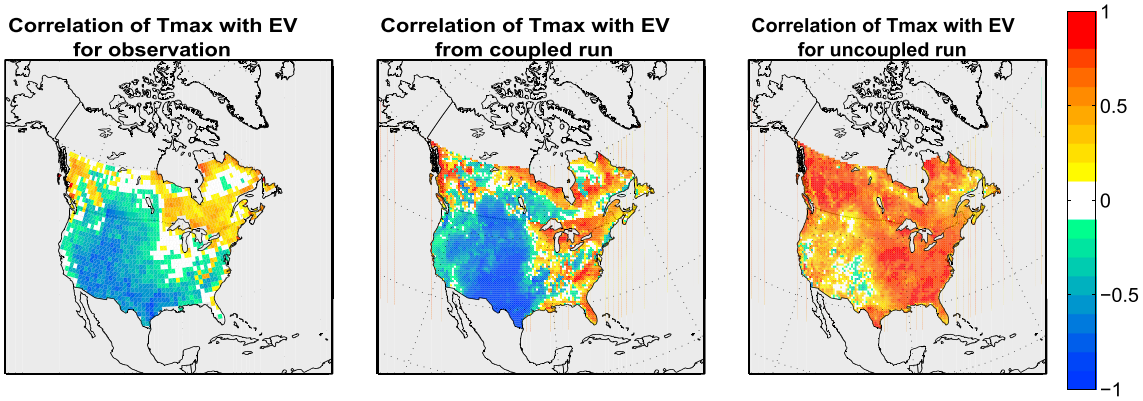

Figure 5. Correlation between evapotranspiration and seasonal mean daily maximum temperature, (left) from observations, (middle) from the coupled, and (right) uncoupled simulations.

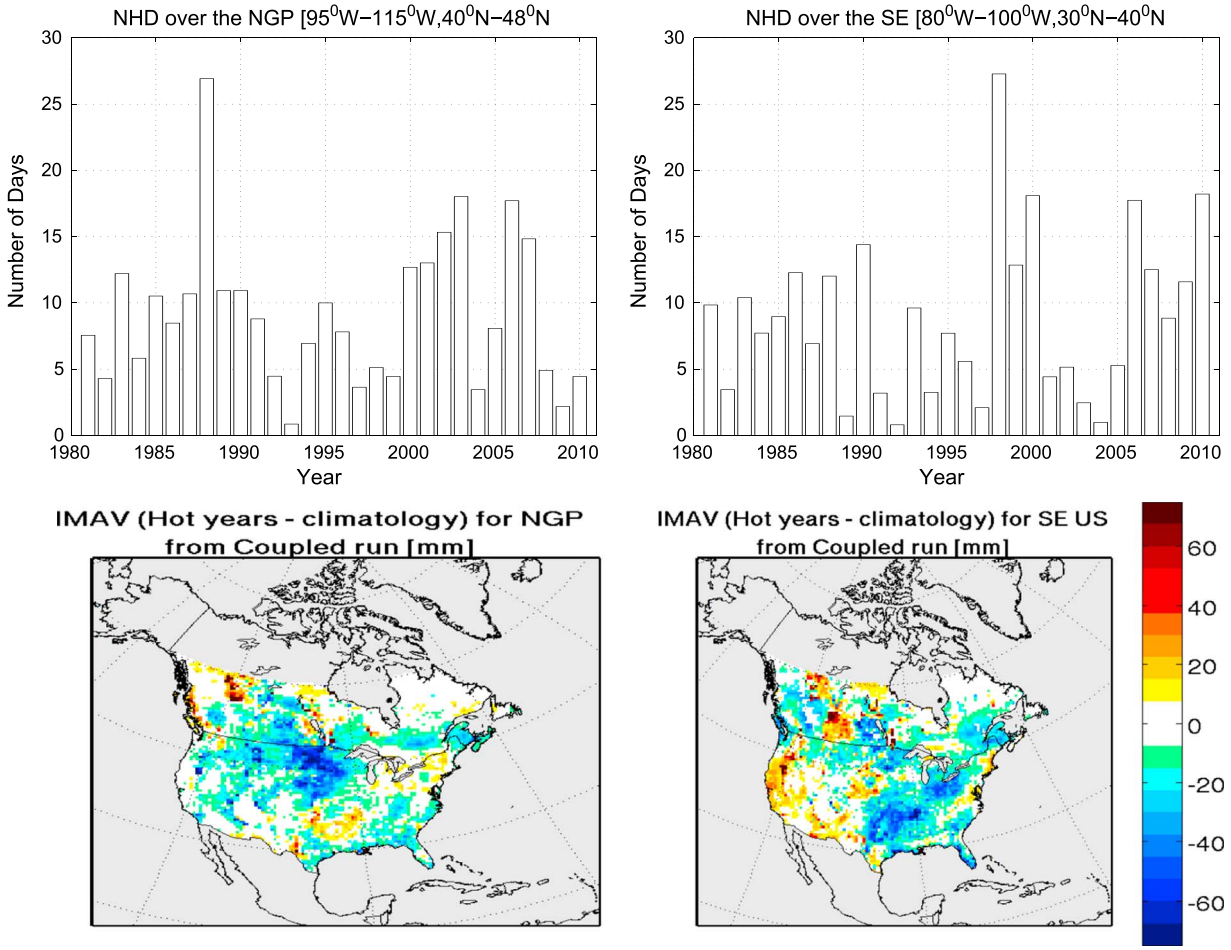

Figure 6. (top row) Average number of hot days for the (left) Northern Great Plains and for the (right) southeast U.S., for the JJA season and for the 1981–2010 period. (bottom row) Composites of JJA vertically integrated soil moisture anomalies (mm); the composites are based on hot years over the (left) Northern Great Plains and (right) southeast U.S.

The figure clearly shows that the correlation values are generally weaker or even positive in the uncoupled simulation, suggestive of lack of soil moisture influence on the variability of temperature. The fact that the strongest negative correlation is located in the transition region between the wet-dry regions, together with the results obtained from GLACE $\Delta\Omega$ and the percentage of variance methods indicate the robustness of the result.

4.1. The Role of Soil Moisture on Temperature Extremes and Hot Spells

The ability of CRCM5 in reproducing the observed NHD and the frequency and maximum duration of hot spells over North America for the 1981–2010 period is evaluated by comparing against these characteristics derived from observation. The analysis focuses on the Northern Great Plains which stands out as a hot spot for soil moisture-temperature coupling. In addition, the southeast U.S. is also selected for this analysis, as this region, according to the variance and correlation methods show some indication of strong coupling.

The number of hot days for these two regions (calculated by averaging the number of hot days at each grid point within the region), for the 1981–2010 JJA period are shown in Figure 6 (top row). Based on this time series, years with the number of hot days above or equal to 15 days are selected for composite analysis. Accordingly, 5 years (1988, 2003, 2006, 2002, and 2007) for the Northern Great Plains (NGP) and 4 years (1998, 2000, 2006, and 2010) for the southeast U.S. are selected for composite analysis.

Figure 7 shows the composites of NHD during summer for the above selected extreme years over the Northern Great Plains and southeast U.S., both for observation and the two CRCM5 simulations. Similar to the observed composites, the coupled simulation reproduces most of the characteristics such as the

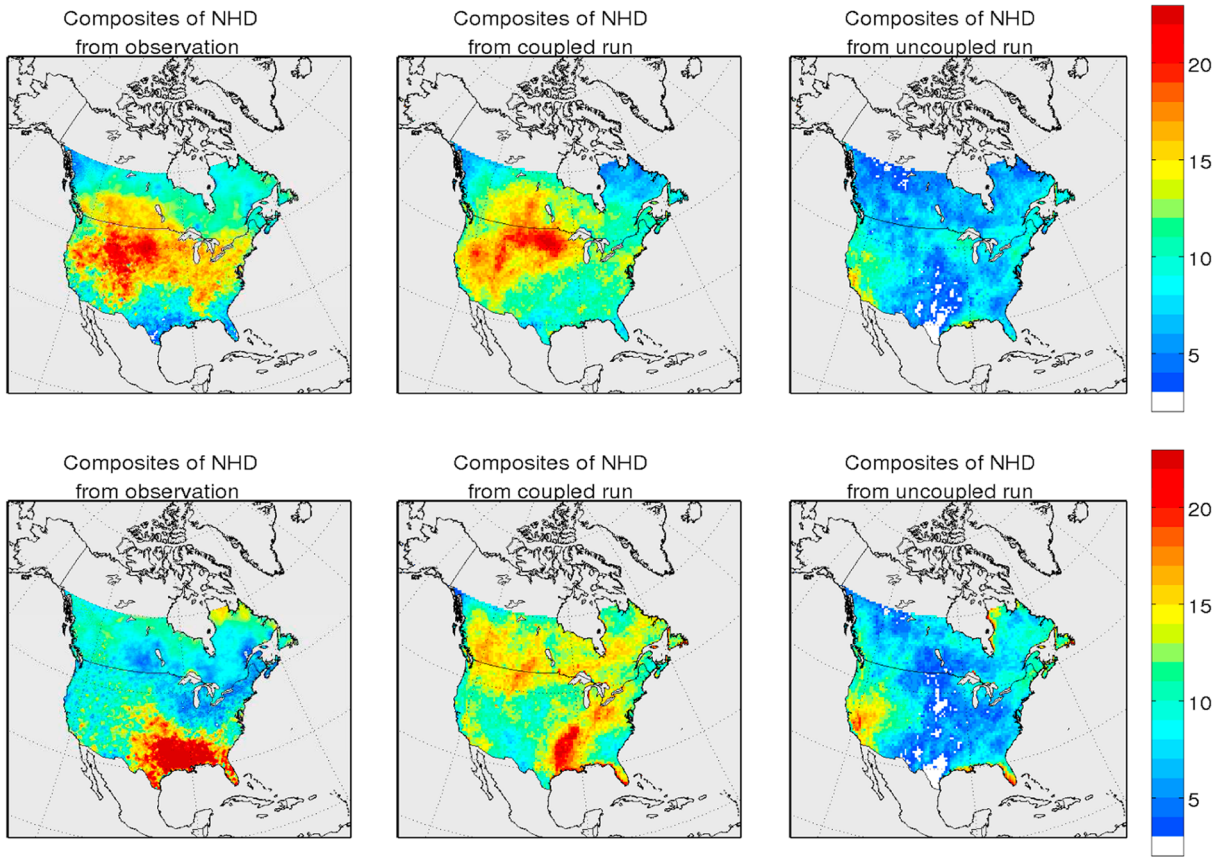

Figure 7. Composites of number of hot days (NHD) greater than the 90th percentile threshold for (left column) observation, (middle column) coupled simulation, and (right column) uncoupled simulation. The threshold values are computed for each calendar day and for each grid point. The composites are based on hot years over the (top row) Northern Great Plains and the (bottom row) Southeast U.S.

location and the spatial distribution of the frequency of hot days, albeit some noticeable differences. For instance, the spatial extent of the region with the highest number of hot days is considerably underestimated over southeast U.S. Similarly, the number of hot days are overestimated over most of southern Canada (Figure 7, bottom row) by the model. Furthermore, the pattern of NHD anomalies (Figure 7) resembles the pattern of negative soil moisture anomalies (Figure 6, bottom row), reaffirming the role of soil moisture interactions in the coupled integration.

Comparing the uncoupled run with the coupled one reveals a significant decrease in NHDs over the whole domain, with the largest decrease being over the Great Plains (from over 22 days in the coupled simulation to the order of 10–12 days in the uncoupled simulations), where the land-atmosphere coupling is stronger. This suggests that the land-atmosphere interaction can modulate (increase in this case) the occurrence of extreme hot days, as uncoupling the land surface from the atmosphere failed to reproduce the NHD, both over the North Great Plains and over the southeast U.S. This once again highlights that interactive soil moisture enhances not only the variability in mean temperature but also the frequency of occurrence of extreme temperature anomalies. These amplifications are stronger over regions of strong land-atmosphere coupling due to the high sensitivity of surface fluxes to soil moisture in these regions.

In order to determine the sensitivity of the studied characteristics of temperature extremes to low soil moisture state, correlation analyses were performed (see Figure 8). This figure indicates significant negative correlations between SPI3 and all extreme temperature indices, notably with NHD over most parts of North America, especially over Northern Great Plains and southeast U.S. The negative correlation of SPI3 with hot days and hot spell indices can be explained as follows. Any precipitation deficit, indicated by low SPI3 values, can lead to decrease in soil moisture. This decrease in soil moisture could cause the rate of evapotranspiration to decrease and hence increases the sensible heat flux, thereby warming the surface and the PBL. One can also in turn suggest that the increase in temperature will enhance the drying of the soil as

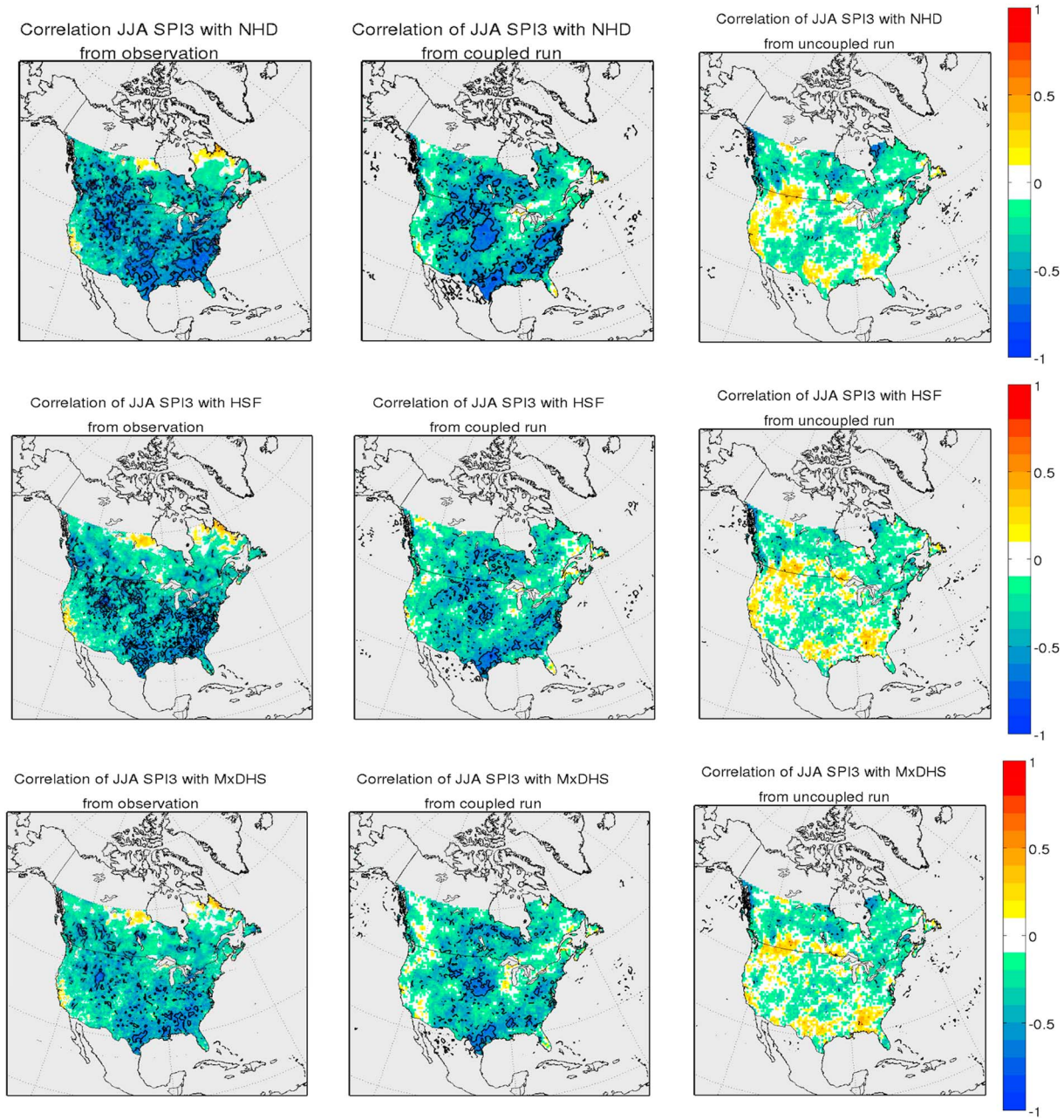

Figure 8. Correlation of JJA SPI3 with the number of (top row) hot days (NHD), (middle row) hot spell frequency (HSF), and (bottom row) maximum duration of hot spells (MxDHS) in summer for (left column) observation, (middle column) coupled simulation, and (right column) uncoupled simulation. Contour lines represent significance at 0.05 level.

this correlation analysis does not provide the causal link. The coupled simulation reproduces the observed spatial patterns of the correlation, although the model tends to underestimate the strength of the relationship between soil moisture (SPI3) and extreme temperature indices. Regions where there is a strong correlation between extreme temperature indices and SPI3 are located over the Great Plains and also over the southeast U.S. Compared to the land-atmosphere coupling hot spots discussed in section 4, the regions identified by this method are more extended and include areas such as the southeastern U.S. as a region where there is a link between soil moisture deficit and extreme hot temperature indices. This result agrees to what *Mueller and Seneviratne* [2012] found using a different observational data set. The uncoupled simulation on the other hand shows a weak (near zero) correlation between SPI3 and the extreme temperature indices. This implies that land-atmosphere coupling is important in reproducing the linkage between soil

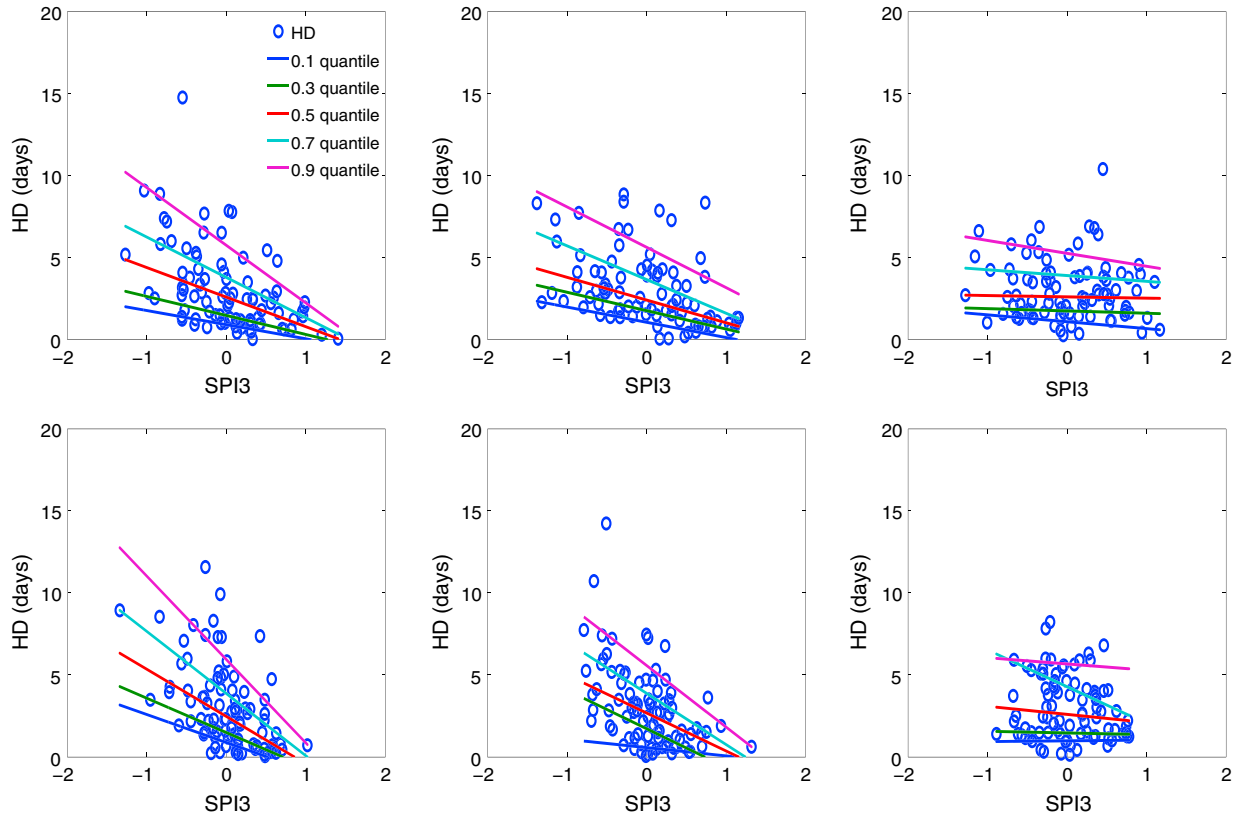

Figure 9. Scatterplot of number of hot days (NHD) versus SPI3 for (top row) Northern Great Plains (NGP) and (bottom row) southeast (SE) U.S. for JJA, from (left column) observations, (middle column) coupled simulation, and (right column) uncoupled simulation. The regression lines correspond to 0.1, 0.3, 0.5, 0.7, and 0.9 quantiles.

moisture and characteristics of temperature extremes. The results also suggest that prolonged soil moisture deficit has more pronounced effect not only on the frequency of hot days and hot spells but also on prolonged duration of hot spells.

The correlation analyses were also repeated with SPI6 (not shown), and the results obtained are similar to that of SPI3, except that correlation values are smaller and regions of significant correlations are much reduced. The additional land-atmosphere hot spot (the southeast U.S.) emerged in the correlation analysis only when extreme events are considered. This implies that for drier conditions with reduced soil moisture (i.e., lower SPI3), the evaporative regime changes from energy limited to moisture limited. In other words, the soil moisture regime shifts from wet to transitional, which is conducive for land-atmosphere coupling and hence can impact the evapotranspiration and subsequently the temperature. This reiterates the fact that the transition zones and hence the land-atmosphere coupling hot spot found in section 4 with the GLACE-type or variance method are not stationary and could change in time. Therefore, climatologically wet/dry zones could become a hot spot, if the surface wetness decreases/increases to a level where evapotranspiration becomes moisture dependent and large enough to affect the climate.

In addition to the above correlation analysis which deals with the mean values of the variables, quantile regression is applied to estimate the relationship between SPI3 and percentage of hot days, similar to *Hirschi et al.* [2010] and *Mueller and Seneviratne* [2012]. This method identifies relationship not only in the mean of the variable's distribution but also in all quantiles of the distribution [*Koenker and Bassett*, 1978]. Figure 9 shows the scatterplot of SPI3 and number of hot days from observations and CRCM5 simulations for the Northern Great Plains (95°W–115°W, 40°N–48°N) and for the southeast U.S. (80°W–100°W, 30°N–40°N) regions. Regression lines are fitted for selected quantiles (0.1, 0.3, 0.5, 0.7, and 0.9). The regression lines derived from observations indicate a strong negative slope for all quantiles suggesting strong influence of SPI on all quantiles of number of hot days. The coupled simulation reproduces these relationships reasonably well, although the slopes of the regression lines are less steep suggesting the model is able to

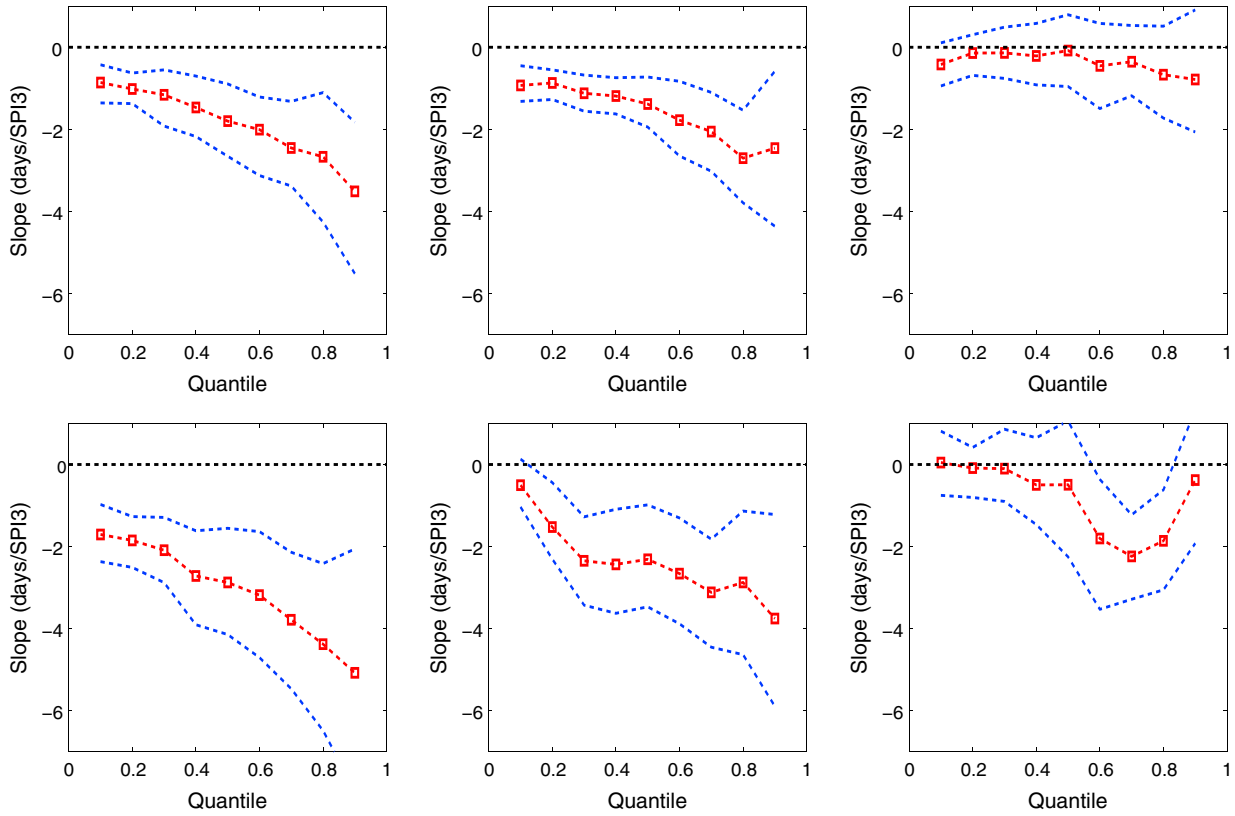

Figure 10. The estimated slope of the quantile regression (red) and its 95% confidence interval (blue line) for (left column) observation, (middle column) coupled simulation, and (right column) uncoupled simulation. (top row) The Northern Great Plains region; (bottom row) the southeast U.S.

reproduce the major aspect of the observed land-atmosphere interaction. The slopes from the uncoupled simulation, on the other hand, are generally lower than those derived from the coupled simulation, which reiterates the importance of soil moisture interaction. Figure 10 shows a gradual increase in the negative slope with increasing quantiles. This implies stronger correlation of higher NHD with drier soil moisture conditions, which was also reported in *Hirschi et al.* [2010] in their study over Europe. The slopes of these quantile regressions, derived from observation and simulations, are significant at the 95% confidence level for most of the quantiles (Figure 10), whereas those derived from the uncoupled simulations are not significant, except for 0.7 quantile for southeast U.S.

5. Soil Moisture-Precipitation Coupling

The impact of soil moisture on precipitation and North American droughts have been investigated in several studies [e.g., *Oglesby and Erickson*, 1989; *Beljaars et al.*, 1996]. As reported by *Lawrence and Slingo* [2005] the process involved in soil moisture-precipitation coupling is more complex than just a local evapotranspiration-precipitation recycling mechanism. There are cascades of processes leading to a positive feedback loop between soil moisture and precipitation via modification of the boundary layer, humidity, and stability [*Eltahir*, 1998; *Schär et al.*, 1999; *Betts*, 2004]. Figure 11 shows the spatial distribution of the soil moisture-precipitation coupling based on $\Delta\Omega$ and percentage of variance methods. From both methods, it is clear that the values of the coupling strength are higher over central and western parts of the continent and smaller over the southeastern coastal area suggesting weaker coupling over the wet areas and stronger coupling over the semiarid areas. The variance and the GLACE methods show slightly different locations of the hot spots. For instance, the GLACE method shows two centers of maxima, one over the central Great Plains and the other over the semiarid regions of the western and southwestern parts of the U.S. The variance method on the other hand emphasizes on a spatially coherent signal over the western part of the U.S. It must be noted that regions that are dry or wet climatologically could in principle occasionally posses a soil moisture anomaly and act as a transitional zone. Generally, the coupling strength is smaller than that of

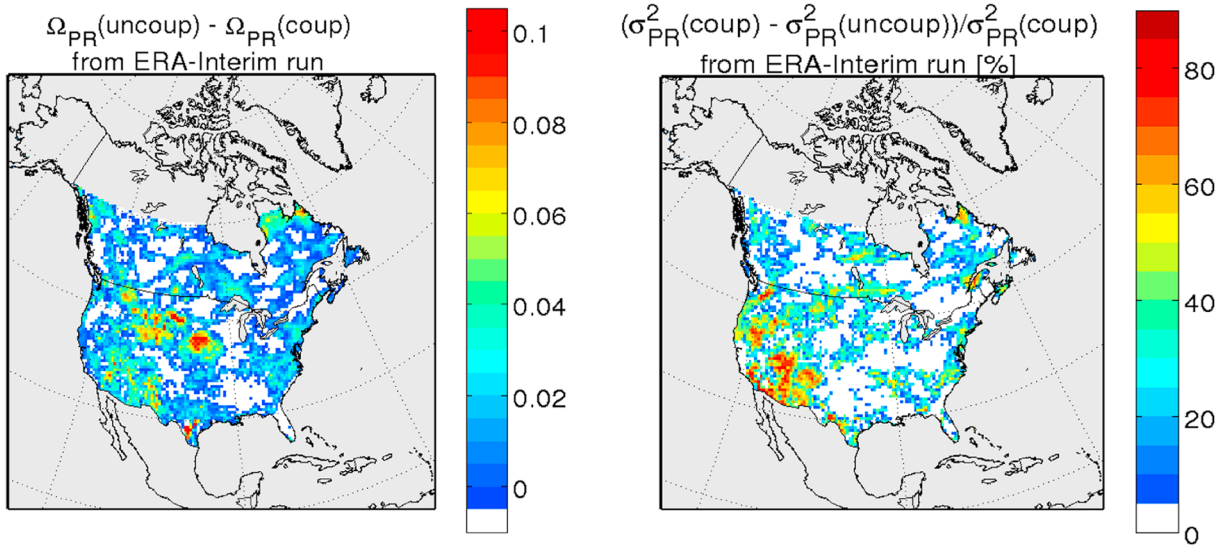

Figure 11. Distribution of (left) GLACE-type coupling strength (Ω_P (uncoupled) − Ω_P (coupled)) and (right) percentage of variance for total precipitation for summer (JJA) season.

the soil moisture-temperature coupling, but this might be due to the fact that precipitation could be more influenced by moisture influx from remote regions via large-scale circulation than through local processes.

To explore this further, the coupling strength is computed for the convective precipitation (cf. see section 2.1 for representation of subgrid-scale convective processes in the model). The results (Figure 12) indicate that the contribution of convective precipitation over the semiarid and arid regions of the west is particularly stronger. Though the $\Delta\Omega$ and the variance method identify the semiarid and arid regions of the western U.S. as a hot spot for soil moisture-convective precipitation coupling, they, however, disagree over some areas such as eastern Canada, where the variance method shows high values of coupling.

One of the main differences between this study and that of the GLACE is that, in the GLACE study, *Koster et al.* [2006] and *Guo et al.* [2006] found that in the multimodel mean plot, the soil moisture-temperature coupling hot spot regions are broadly colocated with the soil moisture-precipitation coupling hot spot regions, whereas in CRCM5 this is not the case. This suggests that the results, among other things, are model dependent in particular to the convection and planetary boundary layer parameterization schemes. This is in addition to the difference in experimental design between this study and the GLACE . For instance, in this study the ensemble members (i.e., the different years) are forced with different sea surface temperatures

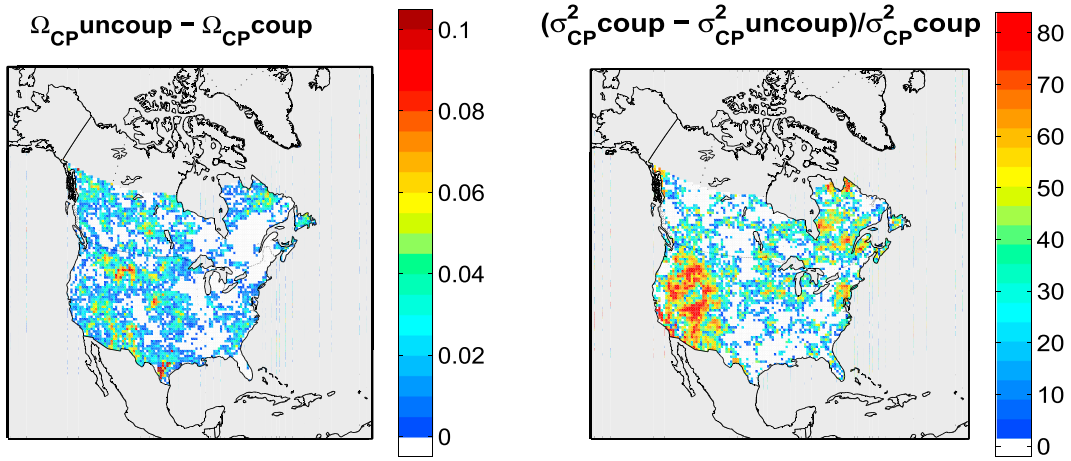

Figure 12. Distribution of coupling strength (left) computed by GLACE method (Ω_{CP}(uncoupled) − Ω_{CP}(coupled)) and (right) using percentage of variance and for convective precipitation for summer (JJA) season.

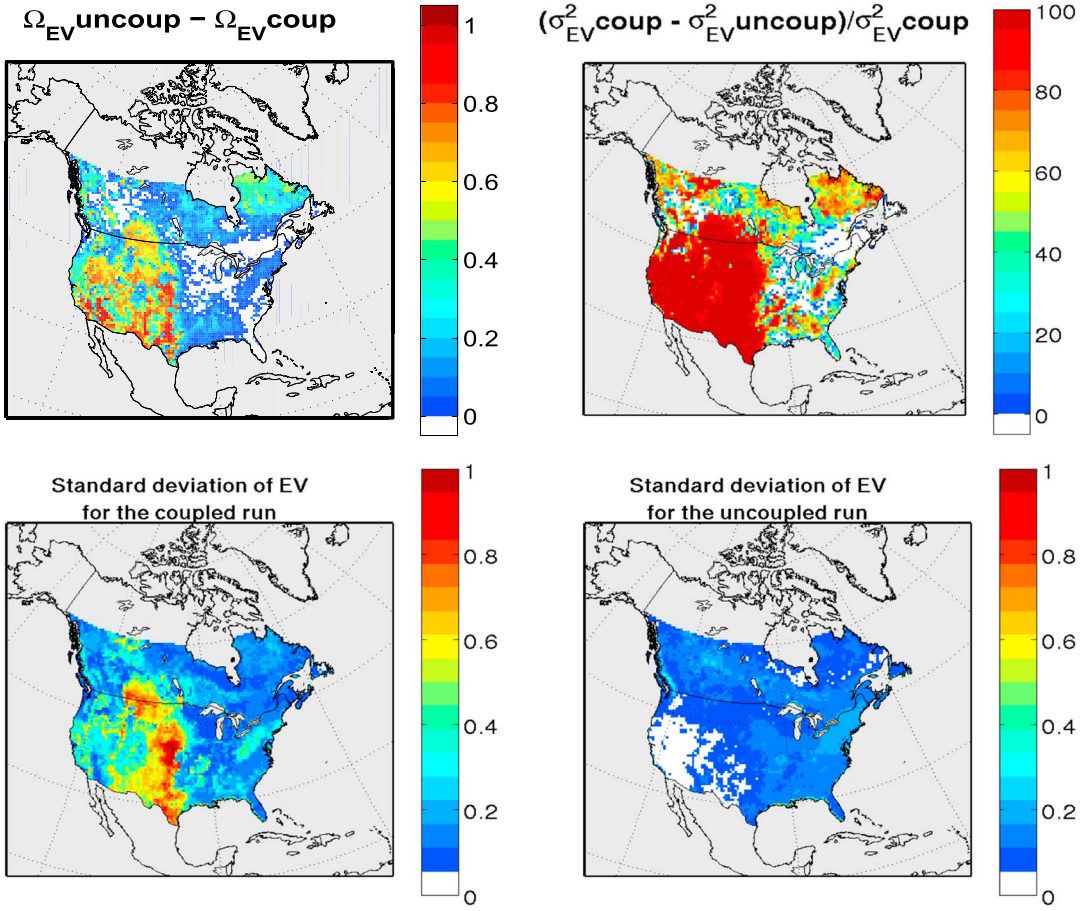

Figure 13. (top row) Coupling strength from (left) GLACE-type coupling strength ($\Delta\Omega_{EV}$), from (right) percentage of variance, and (bottom row) standard deviation of evapotranspiration for the (left) coupled and (right) uncoupled simulations.

(SSTs), while in the GLACE experiment each ensemble member is forced with the same SST (i.e., taken from a single year). It must also be noted that in the GLACE experiment, large differences were noted among the 12 participating GCMs with respect to soil moisture-precipitation coupling hot spots, and the ensemble mean resembles mostly the three models with high value of $\Delta\Omega_p$ over the Great Plains.

We nevertheless investigate the reasons for the weak soil moisture-precipitation coupling in CRCM5. As discussed in *Guo et al.* [2006], *Lawrence and Slingo* [2005], and *Seneviratne et al.* [2010], soil moisture and precipitation are linked via evapotranspiration (EV). Therefore, it will be useful to look at soil moisture-evapotranspiration coupling and evapotranspiration-precipitation link separately.

Figure 13 shows the coupling strength between soil moisture and evapotranspiration and it suggests that there exist strong coupling over the semiarid and arid regions of the central and western U.S. and weaker coupling over the wet eastern part of the study region. The weak coupling strength over the eastern side is also natural because over wet regions evapotranspiration is not controlled by soil moisture, but by radiation [*Seneviratne et al.*, 2010]. Similar results, i.e., strong coupling between soil moisture and evapotranspiration but weaker coupling between soil moisture and precipitation, were also reported by *Lawrence and Slingo* [2005], in their study with the Hadley Centre Atmosphere-only GCM. They argue that for a soil moisture-evapotranspiration coupling to have a strong influence on precipitation, both the coupling strength ($\Delta\Omega_{EV}$) as well as the interannual variability of the evapotranspiration (σ_{EV}) should be large. The spatial pattern of the interannual standard deviation of evapotranspiration is shown in Figure 13 (bottom row) and it is clear that the interannual variability is generally weak, though there is a localized maxima over the Great Plains; a pattern similar to the soil moisture-temperature coupling.

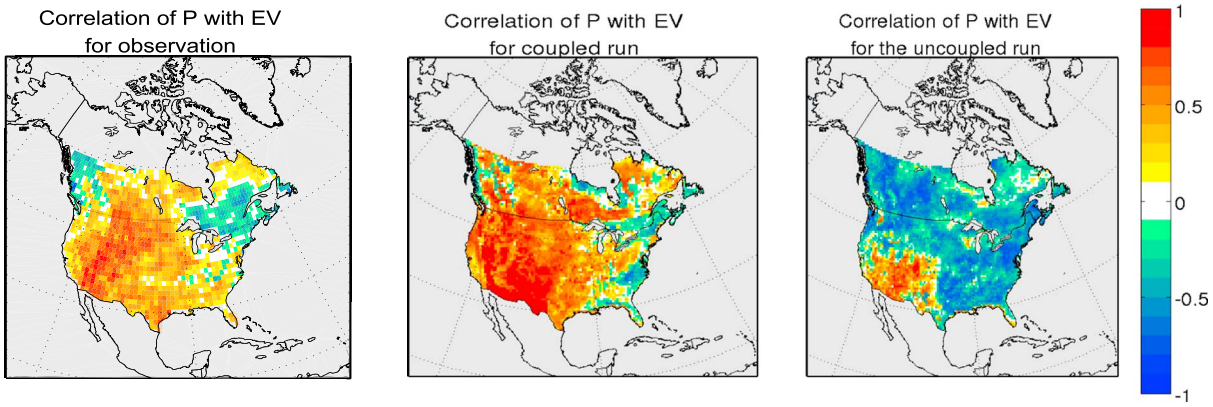

Figure 14. Correlation between evapotranspiration (EV) and total precipitation (P) from (left) observation, (middle) coupled simulation, and (right) uncoupled simulation.

The second part of the soil moisture-precipitation link is the association between evapotranspiration and precipitation. Figure 14 shows the correlation between evaporation and precipitation from the coupled and uncoupled runs. The coupled run shows strong positive correlation over the central and western part of North America, with a maxima over the southwestern part of the U.S. This result suggests that there is a clear linear association between evapotranspiration and precipitation. It does not, however, differentiate whether the high/low evapotranspiration that lead to high/low precipitation is due to local recycling or due to the influx of water vapor (moisture) from remote regions (facilitated by the wet soil to make the atmosphere less stable), which leads to increased precipitation. Further investigation of the indirect effects of soil moisture on precipitation might indicate how the soil moisture could affect the stability of the atmosphere and enhance precipitation, in addition to local recycling. In fact, *Betts* [2004] suggests that land-atmosphere coupling should include cloud and radiation fields, surface partitioning of latent and sensible heat fluxes, boundary layer, and soil moisture.

5.1. Soil Moisture and Extreme Wet Spells

The relationship between land surface condition and extreme precipitation events is analyzed both in observational data set and in CRCM5 simulations. Analysis of the duration and frequency of dry spells in the two CRCM5 (coupled and uncoupled) simulations (not shown) did not show any significant differences between them, suggesting lack of soil moisture influence on the frequency and persistence of extreme dry events in the model. Analysis of extreme wet spells, on the other hand, shows that the duration of extreme wet spells are indeed sensitive to positive soil moisture anomalies. This suggests that the soil moisture interactions with the two extreme (wet and dry) precipitation events are nonlinear. Figure 15 shows the composites of the maximum duration of wet spells from observation and the two CRCM5 simulations. The years to composite are selected by comparing the time series of the average number of consecutive extreme precipitation days for the Northern Great Plains (Figure 15, top). The selected extreme years are 1983, 1992, 1993, 1998, 2009, and 2010. It is interesting that four out of the six extreme years correspond to strong or medium El Niño years (the years 1998 and 1983 are strong positive El Niño–Southern Oscillation (ENSO) years). It is well documented [e.g., *Ropelewski and Halpert*, 1986] that El Niño years are associated with positive rainfall events over western north America, particularly the Great Basins. What we notice here is how regional land-atmosphere interactions and feedbacks interact with large-scale forcings associated with ENSO to amplify and sustain the duration of wet spells. The composites of maximum duration of wet spell (Figure 15) show higher values over the semiarid regions of the western part of the continent, and this spatial pattern is well reproduced in the coupled simulation, although the duration of these extreme wet spells are longer in the model. For the uncoupled simulation, these durations are not only shorter but also not coherently distributed compared to the observation and coupled simulation, suggesting that the land surface processes may have an influence on the persistence of extreme high-precipitation days over the semiarid region of western North America. Land atmosphere interactions and feedbacks over climatologically semiarid regions should not be surprising because when anomalous persistent precipitation occur over these dry regions, the soil moisture regime will shift from dry to transitional state and hence become conducive for land-atmosphere coupling, as the evapotranspiration from this region could now

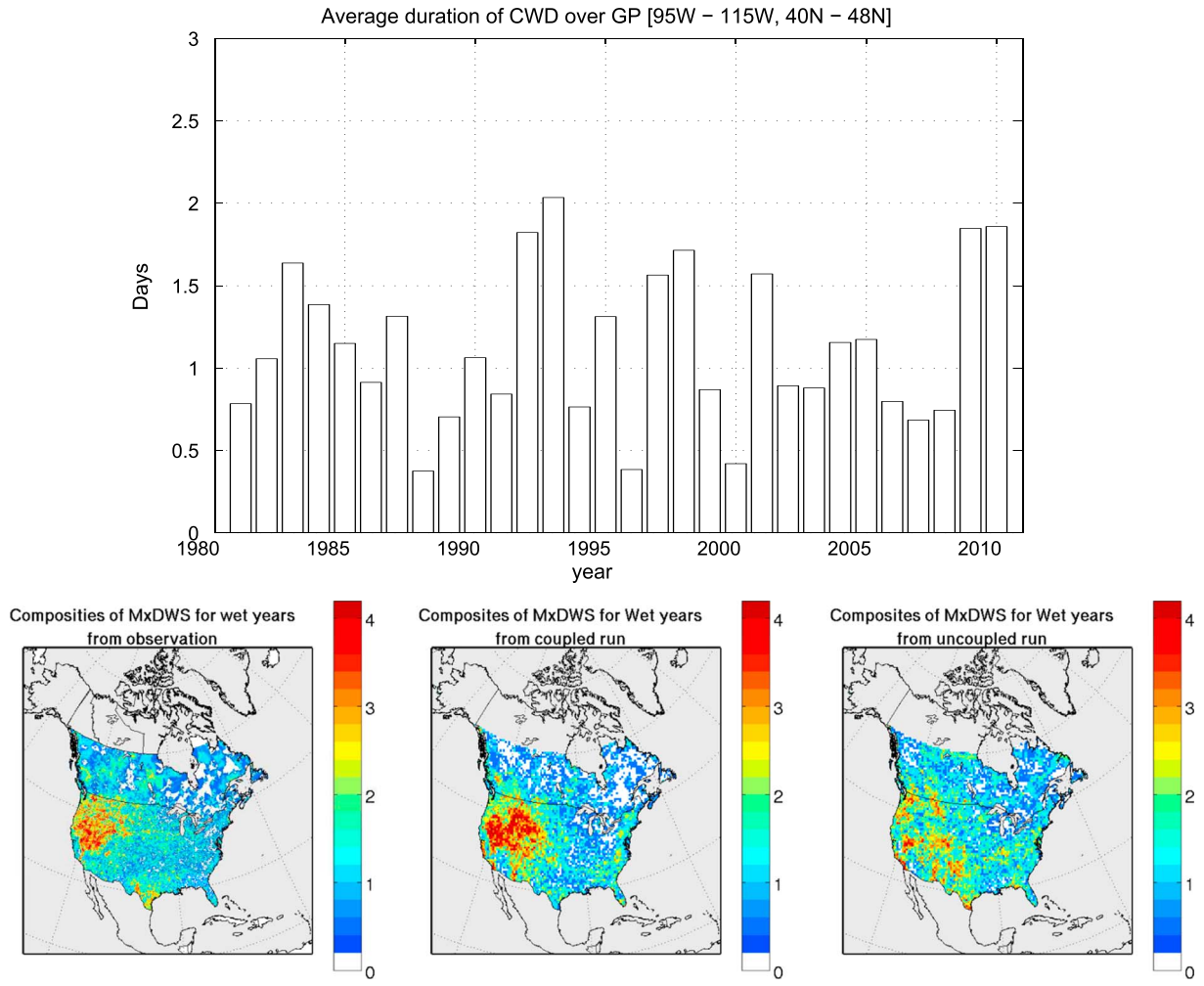

Figure 15. (top) Longest duration of extreme wet spells averaged over the Northern Great Plains from observations. (bottom) Composites of maximum duration of consecutive extreme wet days (MxDWS) (i.e., days with precipitation events greater than the 9th percentile threshold) from (left) observation, (middle) coupled simulation, and (right) uncoupled simulation.

be large enough to affect the climate. Interestingly, this region coincides with the region where the soil moisture-mean summer precipitation (particularly convective) coupling strength is stronger in the model suggesting the land-atmosphere coupling over these semiarid regions are not only affecting the variability but also the duration of extreme wet spells. Positive feedback between soil moisture and precipitation has already been suggested in previous work [e.g., *Eltahir*, 1998] indicating high soil moisture anomalies favor convection instability and rainfall via its impact on the boundary layer temperature, humidity, and the moist static energy.

6. Summary and Conclusions

In this study we analyzed two CRCM5 simulations, one with interactive and the other with prescribed climatological (keeping annual cycle) soil moisture, to examine the extent of land-atmosphere coupling over North America during the summer season. Evaluation of CRCM5 confirms that it is able to reproduce the amount and spatial distribution of the mean and interannual variability of the seasonal mean precipitation and temperature over North America, suggesting the utility of the model for sensitivity study. Analysis of the coupling strength shows that the model identifies the Great Plains of the U.S. and central Canada as a hot spot for the soil moisture-temperature coupling, which is consistent with the GLACE studies. The soil moisture-precipitation coupling on the other hand shows a weak signature and is also extended beyond the Great Plains to the semiarid region of the western part of the continent. Previous studies by *Koster et al.*

[2006] and *Guo et al.* [2006] had indicated Northern and Central Great Plains as soil moisture-precipitation coupling hot spots. As evapotranspiration is one of the major links between soil moisture and precipitation, coupling strength between soil moisture and evapotranspiration is computed to investigate if the weak coupling between soil moisture and precipitation in CRCM5 is due to weak coupling between soil moisture-evapotranspiration or between evapotranspiration and precipitation. Results suggest strong soil moisture-evapotranspiration coupling over the semiarid and arid regions of the central and western parts of the continent. The variability of evapotranspiration in the coupled simulation is, however, found to be generally smaller though the location of maximum variability is colocated with the location of the maxima of the standard deviation of temperature. Strong positive correlation between evapotranspiration and precipitation is also noted for both observation and the coupled simulation. Further analysis is, however, needed to understand the process and mechanisms of soil moisture-precipitation coupling.

Results of the soil moisture-extreme climate analysis show, in addition to the Great Plains, (which were also reported in previous studies), additional hot spots over the wet regions of the southeast U.S. (when the soil moisture anomalies are negative) and over the semiarid regions of the western North America (in the case of positive soil moisture anomaly).

These results are interesting because they demonstrate that the land-atmosphere coupling could become important for climatologically wet/dry areas during extreme dry/wet years when they acquire the characteristics of transitional zone, where evapotranspiration is soil moisture driven and also is large enough to affect the climate.

Acknowledgments

This research was carried out within the framework of the Canadian Network for Regional Climate and Weather Processes (CNRCWP) funded by the National Science and Engineering Research Council (NSERC). The ERA-40 and ERA-Interim reanalysis data used to drive CRCM5 were obtained from the European Centre for Medium-Range Weather Forecasts (ECMWF). The daily maximum temperature and daily precipitation products used in this study for the U.S. are available at http://www.hydro.washington.edu/Lettenmaier/Data/gridded/ and the corresponding data sets over Canada can be obtained from Natural Resources Canada/Agriculture and Agri-Food Canada. The Evapotranspiration data from GLDAS used here are available from http://disc.sci.gsfc.nasa.gov/services/grads-gds/gldas. The CRCM5 code and simulations can be obtained from ESCER Centre, via the corresponding author.

References

Bélair, S., J. Mailhot, C. Girard, and P. Vaillancourt (2005), Boundary layer and shallow cumulus clouds in a medium-range forecast of a large-scale weather system, *Mon. Weather Rev.*, *133*(7), 1938–1960.

Beljaars, A. C., P. Viterbo, M. J. Miller, and A. K. Betts (1996), The anomalous rainfall over the United States during July 1993: Sensitivity to land surface parameterization and soil moisture anomalies, *Mon. Weather Rev.*, *124*(3), 362–383.

Benoit, R., J. Côté, and J. Mailhot (1989), Inclusion of a TKE boundary layer parameterization in the Canadian regional finite-element model, *Mon. Weather Rev.*, *117*(8), 1726–1750.

Betts, A. K. (2004), Understanding hydrometeorology using global models, *Bull. Am. Meteorol. Soc.*, *85*(11), 1673–1688.

Côté, J., S. Gravel, A. Méthot, A. Patoine, M. Roch, and A. Staniforth (1998), The operational CMC-MRB global environmental multiscale (GEM) model. Part I: Design considerations and formulation, *Mon. Weather Rev.*, *126*(6), 1373–1395.

Dee, D., et al. (2011), The ERA-Interim reanalysis: Configuration and performance of the data assimilation system, *Q. J. R. Meteorol. Soc.*, *137*(656), 553–597.

Delage, Y. (1997), Parameterising sub-grid scale vertical transport in atmospheric models under statically stable conditions, *Boundary Layer Meteorol.*, *82*(1), 23–48.

Delworth, T., and S. Manabe (1989), The influence of soil wetness on near-surface atmospheric variability, *J. Clim.*, *2*(12), 1447–1462.

Dirmeyer, P. A., R. D. Koster, and Z. Guo (2006), Do global models properly represent the feedback between land and atmosphere?, *J. Hydrometeorol.*, *7*(6), 1177–1198.

Eltahir, E. A. (1998), A soil moisture–rainfall feedback mechanism: 1. Theory and observations, *Water Resour. Manage.*, *34*(4), 765–776.

Fischer, E., S. Seneviratne, D. Lüthi, and C. Schär (2007a), Contribution of land-atmosphere coupling to recent European summer heat waves, *Geophys. Res. Lett.*, *34*, L06707, doi:10.1029/2006GL029068.

Fischer, E. M., S. Seneviratne, P. Vidale, D. Lüthi, and C. Schär (2007b), Soil moisture-atmosphere interactions during the 2003 European summer heat wave, *J. Clim.*, *20*(20), 5081–5099.

Guo, Z., et al. (2006), GLACE: The global land-atmosphere coupling experiment. Part II: Analysis, *J. Hydrometeorol.*, *7*(4), 611–625.

Hirschi, M., S. I. Seneviratne, V. Alexandrov, F. Boberg, C. Boroneant, O. B. Christensen, H. Formayer, B. Orlowsky, and P. Stepanek (2010), Observational evidence for soil-moisture impact on hot extremes in southeastern Europe, *Nat. Geosci.*, *4*(1), 17–21.

Hopkinson, R. F., D. W. McKenney, E. J. Milewska, M. F. Hutchinson, P. Papadopol, and L. A. Vincent (2011), Impact of aligning climatological day on gridding daily maximum-minimum temperature and precipitation over Canada, *J. Appl. Meteor. Climatol.*, *50*(8), 1654–1665.

Hutchinson, M. F., D. W. McKenney, K. Lawrence, J. H. Pedlar, R. F. Hopkinson, E. Milewska, and P. Papadopol (2009), Development and testing of Canada-wide interpolated spatial models of daily minimum-maximum temperature and precipitation for 1961-2003, *J. Appl. Meteor. Climatol.*, *48*(4), 725–741.

Jaeger, E., and S. Seneviratne (2011), Impact of soil moisture–atmosphere coupling on European climate extremes and trends in a regional climate model, *Clim. Dyn.*, *36*(9–10), 1919–1939.

Jeong, D. I., L. Sushama, and M. N. Khaliq (2014), The role of temperature in drought projections over North America, *Clim. Change*, doi:10.1007/s10584-014-1248-3.

Kain, J., and J. Fritsch (1992), The role of the convective trigger function in numerical forecasts of mesoscale convective systems, *Meteorol. Atmos. Phys.*, *49*(1–4), 93–106.

Karl, T. R. (1986), The relationship of soil moisture parameterizations to subsequent seasonal and monthly mean temperature in the United States, *Mon. Weather Rev.*, *114*(4), 675–686.

Koenker, R., and G. Bassett Jr. (1978), Regression quantiles, *Econometrica*, *46*, 33–50.

Koster, R. D., et al. (2006), GLACE: The Global Land-Atmosphere Coupling Experiment. Part I: Overview, *J. Hydrometeorol.*, *7*(4), 590–610.

Lawrence, D. M., and J. M. Slingo (2005), Weak land-atmosphere coupling strength in HadAM3: The role of soil moisture variability, *J. Hydrometeorol.*, *6*(5), 670–680.

Li, J., and H. Barker (2005), A radiation algorithm with correlated-k distribution. Part I: Local thermal equilibrium, *J. Atmos. Sci.*, *62*(2), 286–309.

Lorenz, R., E. Davin, and S. Seneviratne (2012), Modeling land-climate coupling in Europe: Impact of land surface representation on climate variability and extremes, *J. Geophys. Res.*, *117*, D20109, doi:10.1029/2012JD017755.
Martynov, A., L. Sushama, R. Laprise, K. Winger, and B. Dugas (2012), Interactive lakes in the Canadian regional climate model, version 5: The role of lakes in the regional climate of North America, *Tellus A*, *64*, 16,226.
Martynov, A., R. Laprise, L. Sushama, K. Winger, L. Šeparović, and B. Dugas (2013), Reanalysis-driven climate simulation over Cordex North America domain using the Canadian regional climate model, version 5: Model performance evaluation, *Clim. Dyn.*, *41*, 2973–3005.
Masson, V., J. L. Champeaux, F. Chauvin, C. Meriguet, and R. Lacaze (2003), A global database of land surface parameters at 1-km resolution in meteorological and climate models, *J. Clim.*, *16*(9), 1261–1282.
Maurer, E., A. Wood, J. Adam, D. Lettenmaier, and B. Nijssen (2002), A long-term hydrologically based dataset of land surface fluxes and states for the conterminous United States*, *J. Clim.*, *15*(22), 3237–3251.
McKee, T. B., N. J. Doesken, and J. Kleist (1993), The relationship of drought frequency and duration to time scales, in *Proceedings of the 8th Conference on Applied Climatology*, vol. 17, pp. 179–183, Am. Meteorol. Soc., Boston, Mass.
Mei, R., G. Wang, and H. Gu (2013), Summer land–atmosphere coupling strength over the United States: Results from the regional climate model RegCM4–CLM3. 5, *J. Hydrometeorol.*, *14*(3), 946–962.
Mironov, D., S. Golosov, E. Heise, E. Kourzeneva, B. Ritter, N. Sceider, and A. Terzhevik (2005), FLake—A lake model for environmental applications, paper presented at 9th Workshop on Physical Processes in Natural Waters, Lancaster Univ. U. K., 4–6 Sept.
Mironov, D., E. Heise, E. Kourzeneva, B. Ritter, N. Schneider, and A. Terzhevik (2010), Implementation of the lake parameterisation scheme flake into the numerical weather prediction model Cosmo, *Boreal Environ. Res.*, *15*, 218–230.
Mueller, B., and S. I. Seneviratne (2012), Hot days induced by precipitation deficits at the global scale, *Proc. Natl. Acad. Sci.*, *109*(31), 12,398–12,403.
Oglesby, R. J., and D. J. Erickson III (1989), Soil moisture and the persistence of North American drought, *J. Clim.*, *2*(11), 1362–1380.
Rodell, M., et al. (2004), The global land data assimilation system, *Bull. Am. Meteorol. Soc.*, *85*(3), 381–394.
Ropelewski, C. F., and M. S. Halpert (1986), North American precipitation and temperature patterns associated with the El Niño/Southern Oscillation (ENSO), *Mon. Weather Rev.*, *114*(12), 2352–2362.
Schär, C., D. Lüthi, U. Beyerle, and E. Heise (1999), The soil-precipitation feedback: A process study with a regional climate model, *J. Clim.*, *12*(3), 722–741.
Seneviratne, S. I., D. Lüthi, M. Litschi, and C. Schär (2006), Land–atmosphere coupling and climate change in Europe, *Nature*, *443*(7108), 205–209.
Seneviratne, S. I., T. Corti, E. L. Davin, M. Hirschi, E. B. Jaeger, I. Lehner, B. Orlowsky, and A. J. Teuling (2010), Investigating soil moisture–climate interactions in a changing climate: A review, *Earth Sci. Rev.*, *99*(3), 125–161.
Sundqvist, H., E. Berge, and J. E. Kristjánsson (1989), Condensation and cloud parameterization studies with a mesoscale numerical weather prediction model, *Mon. Weather Rev.*, *117*(8), 1641–1657.
Tawfik, A. B., and A. L. Steiner (2011), The role of soil ice in land-atmosphere coupling over the United States: A soil moisture–precipitation winter feedback mechanism, *J. Geophys. Res.*, *116*, D02113, doi:10.1029/2010JD014333.
Taylor, C. M., F. Saïd, and T. Lebel (1997), Interactions between the land surface and mesoscale rainfall variability during HAPEX-Sahel, *Mon. Weather Rev.*, *125*(9), 2211–2227.
Verseghy, D. (2009), CLASS the Canadian land surface scheme (version 3.4), *Tech. Rep.*, Climate Research Division, Science and Technology Branch, Environment Canada, p. 107.
Verseghy, D., N. McFarlane, and M. Lazare (1993), CLASS-A Canadian land surface scheme for GCMs, II. Vegetation model and coupled runs, *Int. J. Climatol.*, *13*(4), 347–370.
Verseghy, D. L. (1991), CLASS-A Canadian land surface scheme for GCMs. I. Soil model, *Int. J. Climatol.*, *11*(2), 111–133.
van den Hurk, B., M. Best, P. Dirmeyer, A. Pitman, J. Polcher, and J. Santanello (2011), Acceleration of land surface model development over a decade of GLASS, *Bull. Am. Meteorol. Soc.*, *92*, 1593–1600.
Walsh, J. E., W. H. Jasperson, and B. Ross (1985), Influences of snow cover and soil moisture on monthly air temperature, *Mon. Weather Rev.*, *113*(5), 756–768.
Zadra, A., R. McTaggart-Cowan, and M. Roch (2012), *Recent Changes to the Orographic Blocking*. Seminar presentation, RPN, Dorval, Canada, 30 March.
Zhang, J., W. C. Wang, and L. R. Leung (2008), Contribution of land-atmosphere coupling to summer climate variability over the contiguous United States, *J. Geophys. Res.*, *113*, D22109, doi:10.1029/2008JD010136.